Journal of Power Sources 218 (2012) 250–253

Contents lists available at SciVerse ScienceDirect

Journal of Power Sources

journal homepage: www.elsevier.com/locate/jpowsour

Short communication

Synthesis and characterization of carbon-coated $LiMnPO_4$ and $LiMn_{1-x}Fe_xPO_4$ ($x = 0.2, 0.3$) materials for lithium-ion batteries

Libero Damen, Francesca De Giorgio, Simone Monaco, Federico Veronesi, Marina Mastragostino*

University of Bologna, Department of Metal Science, Electrochemistry and Chemical Techniques, Via San Donato 15, 40127 Bologna, Italy

HIGHLIGHTS

- C-$LiMn_{1-x}Fe_xPO_4$ ($x = 0$, 0.2, 0.3) were synthesized via a cost-effective procedure.
- $LiMnPO_4$ from totally soluble precursors provided an attractive C-coated material.
- The best performing electrodes are based on $LiMnPO_4$ and $LiMn_{0.8}Fe_{0.2}PO_4$.

ARTICLE INFO

Article history:
Received 22 February 2012
Received in revised form
16 June 2012
Accepted 27 June 2012
Available online 7 July 2012

Keywords:
High-voltage cathode
Lithium-ion battery
$LiMn_{1-x}Fe_xPO_4$
$LiMnPO_4$

ABSTRACT

Structural, morphological and electrochemical characterizations in EC:DMC-$LiPF_6$ of carbon-coated $LiMnPO_4$ and $LiMn_{1-x}Fe_xPO_4$ ($x = 0.2$, 0.3) cathode materials synthesized via a cost-effective procedure based on sol–gel (from partially or totally soluble precursors in water), pyrolysis and ball milling steps are reported. Carbon-coated $LiMnPO_4$ obtained from totally soluble precursors featuring at 0.1 C 125 $mAhg^{-1}$ at 50 °C and 95 $mAhg^{-1}$ at 30 °C, with a capacity fade per cycle of 0.5% at 50 °C and 0.4% at 30 °C, is a very promising material, particularly in consideration of the inexpensive procedure that was pursued for its synthesis.

© 2012 Elsevier B.V. All rights reserved.

1. Introduction

Lithium transition metal phosphates are attractive cathode materials for rechargeable lithium-ion batteries because of the high chemical and thermal stability and the low cost of their precursors. The extensive enhancement in cathode performance of $LiFePO_4$ has stimulated the search for other olivines as $LiMnPO_4$. $LiMnPO_4$ is a more advantageous material than $LiFePO_4$ in terms of battery energy density because of its high working voltage, 4.1 V *vs.* Li instead of 3.5 V and the same theoretical capacity, 170 mAh g^{-1} [1,2]. However, the delivered capacity and the cycling stability of lithium manganese phosphate are still lower than those of lithium iron phosphate. This is due to the poor Li^+ insertion/deinsertion kinetics because of the Jahn–Teller lattice deformation and the structural changes of $LiMnPO_4$ during cycling [3]. Several approaches have been proposed to improve electrochemical performance of $LiMnPO_4$: preparing micro-, nano-sized and platelet like particles to reduce Li^+ diffusion length [4–11], coating particles with a carbon layer [11–13] and doping $LiMnPO_4$ with cations (Co, Mg, Ti, Zr, V, Fe, Gd and Zn) [14,15]. Increasing in electrochemical performance was achieved when some Mn ions were replaced with Fe to form solid solutions $LiMn_{1-x}Fe_xPO_4$ [1,16,17].

We report the results of the structural, morphological and electrochemical characterization of carbon-coated $LiMn_{1-x}Fe_xPO_4$ ($x = 0$, 0.2, 0.3) synthesized via a procedure based on sol-gels from different precursors, and pyrolysis and ball milling steps, a cost-effective procedure for mass production of materials. The electrochemical characterization of the electrodes was performed in cells *vs.* Li in EC:DMC- $LiPF_6$ electrolyte.

2. Experimental

The chemicals for the syntheses were H_3PO_4, Li_3PO_4, $MnCO_3$, Fe(II) oxalate dihydrate and Mn (II) acetate tetrahydrate (Sigma–Aldrich), and $LiOH \cdot H_2O$ and citric acid monohydrate (Fluka). The gel pyrolyses were performed in a Carbolite tube

* Corresponding author. Tel.: +39 051 2099798; fax: +39 051 2099365.
E-mail address: marina.mastragostino@unibo.it (M. Mastragostino).

0378-7753/$ – see front matter © 2012 Elsevier B.V. All rights reserved.
http://dx.doi.org/10.1016/j.jpowsour.2012.06.090

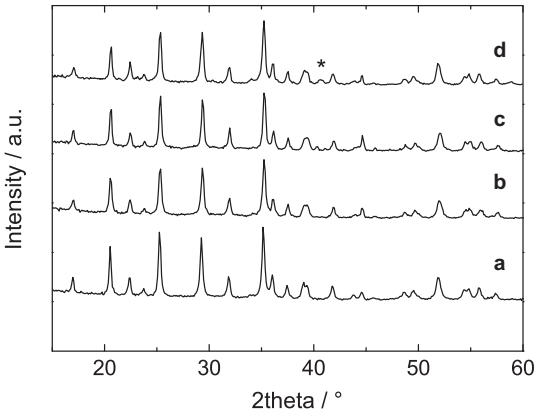

Fig. 1. XRD patterns of all materials: (a) M100(I), (b) MF8020(I), (c) MF7030(I), and (d) M100(II).

furnace, and the planetary mill used to grind the synthesized powders was a Pulverisette 6 Fritsch. The XRD analysis was performed by a Philips X'pert diffractometer, a Cu Kα (λ = 1.5406 Å) radiation source and Ni filter with continuous acquisition in 10–80° 2θ range, 0.05° 2θ s^{-1} scan rate. The thermo-gravimetric analysis was carried out with a TGA TA Q50 from room temperature (RT) to 700 °C (heating- rate 10 °C min^{-1}) in O_2 flux. The scanning electron microscopy (SEM) images were acquired with a Zeiss EVO 50. High resolution transmission electron microscopy (HRTEM) images were obtained by a JEOL-JEM 2010 Electron Microscope equipped with an X-EDS analysis system.

Electrochemical characterization of the synthesized materials was carried out on composite electrodes prepared by "doctor-blade" technique. A slurry with 85 wt.% synthesized materials, 10 wt.% conductive carbon (SuperP, Erachem) and 5 wt.% PVDF (Kynar HSV 900) was prepared in a IKA Ultra-Turrax Tube Dispenser and coated onto etched aluminum foil current collector using a mini coating machine (MC 20, Hohsen Corp.) and dried at 120 °C for 2 h. Circular electrodes were cut from the foil with a geometric area of 0.64 cm^2, pressed at 3000 psi (ICL-12, Ton EZ-Press) and dried at 150 °C under vacuum overnight. The composite mass loading was in the 3–8 mg per cm^2 range of geometric area. "Swagelok-type" electrochemical cells with Li reference electrode were used for electrode characterization in cell *vs*. Li with Li in excess. A dried and degassed glass separator (Whatman GF/D 400 μm thick) was used after soaking in the same electrolyte of the electrochemical cell ethylene carbonate (EC): dimethylcarbonate (DMC) 1:1–1 M $LiPF_6$ (Merck LP30). Cell assembly and sealing were performed in an argon atmosphere MBraun Labmaster 130 dry box (H_2O and $O_2 < 1$ ppm) and the electrochemical tests were performed by Perkin–Elmer VMP multichannel potentiostat. All the reported potentials are referred to the reference Li electrode and the specific capacity data are referred to the mass of the olivine in the electrode.

3. Results and discussion

3.1. Synthesis and characterization

$LiMn_{0.8}Fe_{0.2}PO_4$ and $LiMn_{0.7}Fe_{0.3}PO_4$ were prepared by sol–gel step from partially water soluble precursors and the final products were indicated MF8020(I) and MF7030(I). For synthesis of $LiMnPO_4$, two different sol-gels from partially soluble precursors (I) and totally soluble (II) for a better precursors' dispersion were performed and the final materials were indicated M100(I) and M100(II). Precursors for M100(I) were $MnCO_3$, H_3PO_4, Li_3PO_4 and citric acid monohydrate ($C_6H_8O_7 \cdot H_2O$), for M100(II) were $Mn(CH_3COO)_2 \cdot 4H_2O$, $LiOH \cdot H_2O$, H_3PO_4 and $C_6H_8O_7 \cdot H_2O$, for MF8020(I) and MF7030(I) were $MnCO_3$, $Fe(C_2O_4) \cdot 2H_2O$, H_3PO_4, Li_3PO_4 and $C_6H_8O_7 \cdot H_2O$. All the precursors were added to water in stoichiometric molar ratio, with exclusion of $C_6H_8O_7 \cdot H_2O$ which for the M100(II) synthesis was 2:1 to enhance cation chelating effect and source of carbon-coating. The aqueous systems were heated at 100 °C to rapidly evaporate water and to obtain dry gels. The gels were ground with mortar and pestle and then pyrolyzed in furnace in argon flow (ca. 200 ml min^{-1}) for 1 h at 700 °C (heating rate 20 °C min^{-1}). Ar/H_2 (95/5%) gases, was originally used to preserve the product from oxidation but proved unnecessary. The resulting black powders were further ground by wet (water or acetone) ball milling in WC jar with 20 balls of 10 mm diameter at 300 rpm for 6 h.

All the powders were characterized by XRD, SEM and TGA. Fig. 1 shows the X-ray patterns: the peaks are all related to the expected product, demonstrating the efficacy of the synthesis procedure, with the exclusion of the small peak at 40.6° 2θ due to manganese oxide impurity for M100(II). The crystallite size of $LiMnPO_4$ powder obtained from totally soluble precursors was 28 nm, smaller than those of other products prepared from partially soluble precursors which ranged from 34 to 43 nm, as evaluated by Scherrer's equation from the XRD 020 peak, and this might positively affect the electrochemical performance.

The carbon content in each powder was evaluated by TGA by heating the samples in O_2 flux from RT up to 700 °C. The oxygen burns off the carbon leaving $LiMnPO_4$ from the carbon coated $LiMnPO_4$ sample and $LiMnPO_4$, $Li_3Fe_2(PO_4)_3$ and Fe_2O_3 from the carbon-coated $LiMn_{1-x}Fe_xPO_4$ ($x > 0$) samples [2]. The samples showed the following carbon content: 6 wt.% M100(I), 9 wt.% MF7030(I), 11 wt.% MF8020(I) and 14 wt.% M100(II).

Fig. 2 reports the SEM images of the synthesized MF8020(I) and M100(II) powders after ball milling; these images show quite large aggregates constituted in turn by small particles (<1 μm). Fig. 3 which shows the HRTEM image of the M100(II) powder with two areas analyzed with X-EDS confirms that a carbon coating is formed on the $LiMnPO_4$ particles.

3.2. Electrochemical tests

The electrochemical characterization of M100(I), MF8020(I) and MF7030(I) composite electrodes based on materials from synthesis

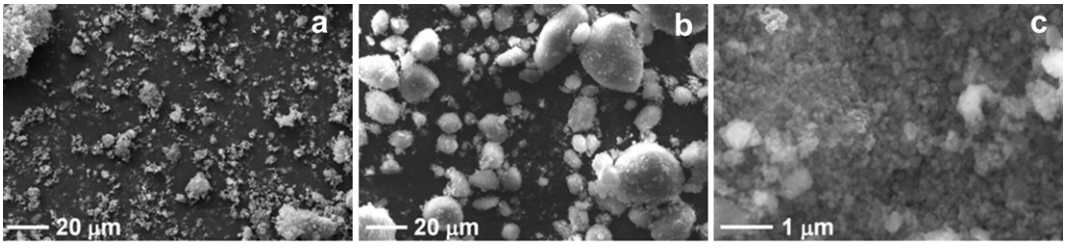

Fig. 2. SEM images of ball milled powders: a) MF8020(I) at 2000X; b) M100(II) at 2000X and c) M100(II) at 50,000X.

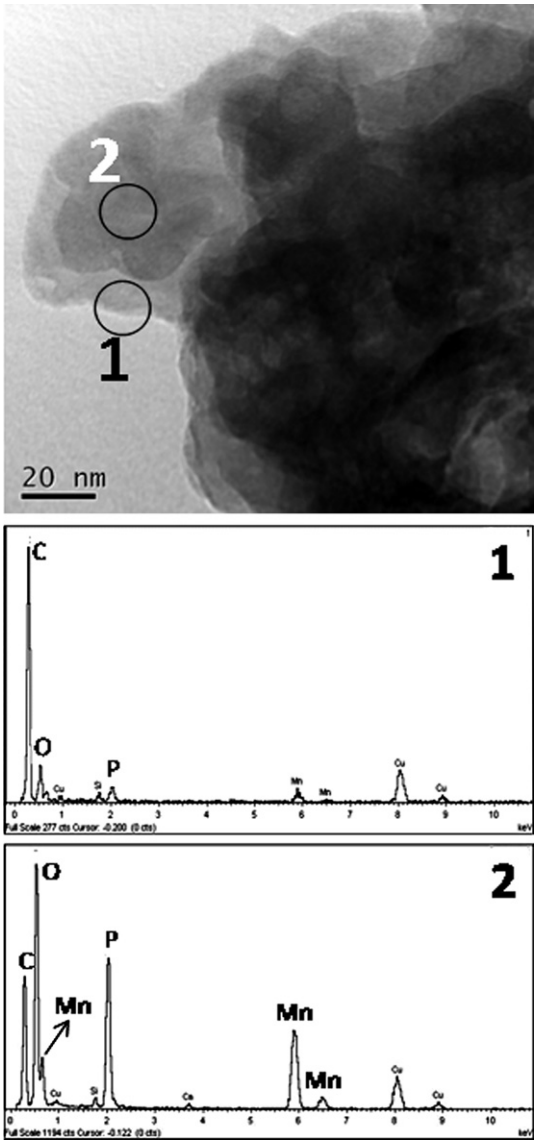

Fig. 3. HRTEM image of M100(II) with two areas analyzed by X-EDS.

I was carried-out by galvanostatic/potentiostatic charge (CC-CV) and galvanostatic discharge cycles (CC) at 30° and 50 °C. The CC was at 0.1 C up to 4.4 V, followed by CV with current cut off at 0.05 C; the cells were discharged down to 2.3 V at 0.1 C. Fig. 4 shows the first discharge curves at 0.1 C and 50 °C of fully charged electrodes demonstrating, according to Yamada [16], that coexistence of Fe and Mn is important for enhancing capacity. Electrode MF8020(I) at the first cycle delivered 135 mAh g^{-1} with a columbic efficiency of ca. 80% increasing to ca. 95% in the subsequent cycles. To evaluate discharge capability of MF8020(I), the electrode was fully charged, and discharged at different C-rates from 0.1 C to 2 C, at 50 °C, and the results are shown in Fig. 5. At the highest C-rate the delivered capacity is 80 mAh g^{-1}, a good value for a manganese-iron phosphate electrode with a total carbon content of ca. 20%. The cycling stability of electrodes, M100(I), MF8020(I) and MF7030(I), was tested by charge (CC-CV)-discharge (CC) at 0.1 C and at 50 °C, and Fig. 6 shows their stability over ten cycles.

Electrochemical tests of M100(II) composite electrode based on $LiMnPO_4$ from synthesis II were performed by CC (0.1 C up to 4.6 V)-CV (0.05 C) charge and CC discharge (down to 2.5 V) at various C-rates

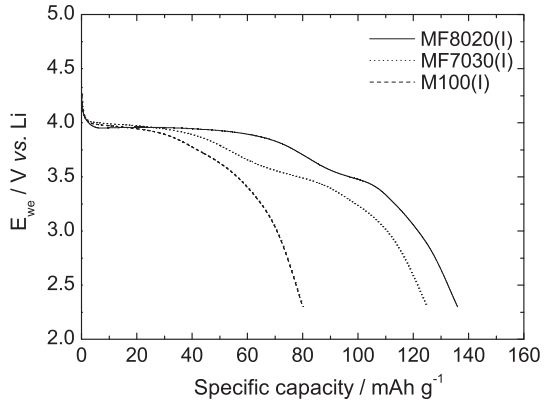

Fig. 4. First CC discharge curves at 0.1 C-rate and 50 °C of M100(I), MF8020(I) and MF7030(I) fully charged electrodes (CC-CV).

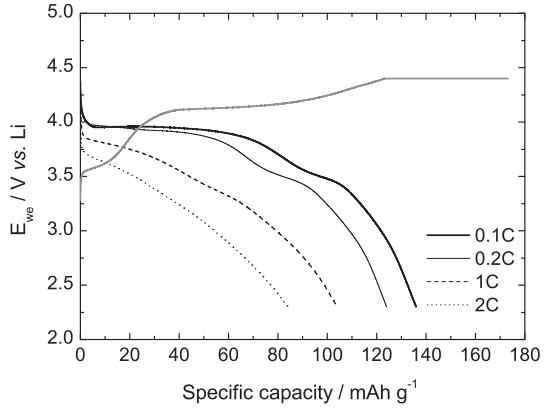

Fig. 5. Discharge capability from 0.1 C to 2 C of fully charged MF8020(I) electrode, at 50 °C.

from 0.1 C to 2 C, at 50 °C, and the results are in Fig. 7. At 2 C the M100(II) delivered 100 mAh g^{-1}, an interesting value for $LiMnPO_4$ at this C-rate. After discharge capability test the same cell was tested to evaluate its charge capability by CC charge (up to 4.6 V) at various C-rates from 0.1 C to 2 C and CC discharge at 0.1 C (down to 2.5 V), at 50 °C, and the results are in Fig. 8. A stored charge of 65 mAh g^{-1} at the high C-rate of 2 C is a good result for such material.

Stability tests on M100(II) electrode were performed at two temperatures, 50° and 30 °C, by CC (0.1 C up to 4.6 V)-CV (0.05 C)

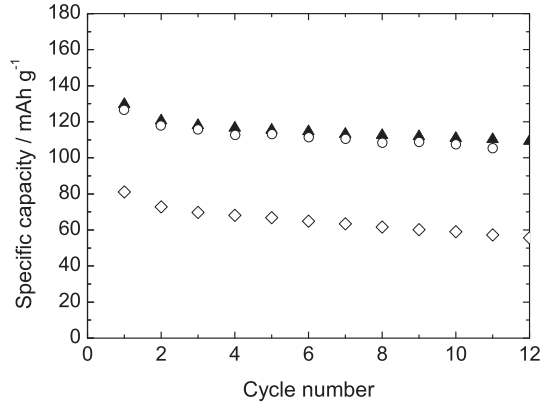

Fig. 6. Specific discharge capacity at 0.1 C and 50 °C *vs.* cycle number of (◇) M100(I), (▲) MF8020(I) and (○) MF7030(I) electrodes.

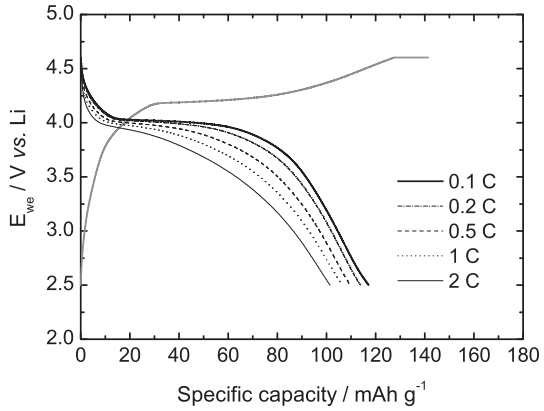

Fig. 7. Discharge capability from 0.1 C to 2 C of fully charged M100(II) electrode at 50 °C.

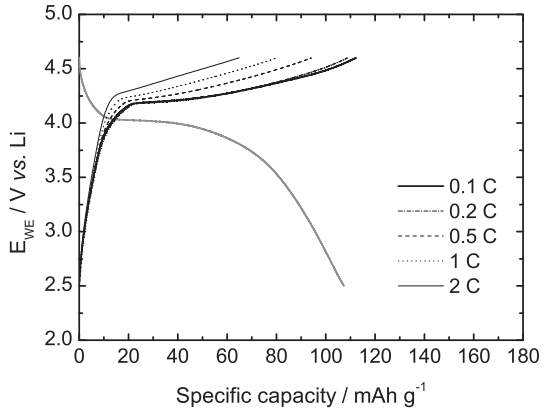

Fig. 8. Charge capability from 0.1 C to 2 C of M100(II) electrode at 50 °C; discharge at 0.1 C.

charge and CC discharge (down to 2.5 V) at 0.1 C. The results in Fig. 9 demonstrate the good stability of the M100(II) electrodes over 50 cycles at both temperatures with coulombic efficiency values at the first cycle of 70–80% increasing to 93–94% in the subsequent cycles. The M100(II) performs better than M100(I), and comparable to the iron-containing MF8020(I), demonstrating the efficacy of the synthesis II of $LiMnPO_4$ from completely soluble precursors and with the highest amount of citric acid which

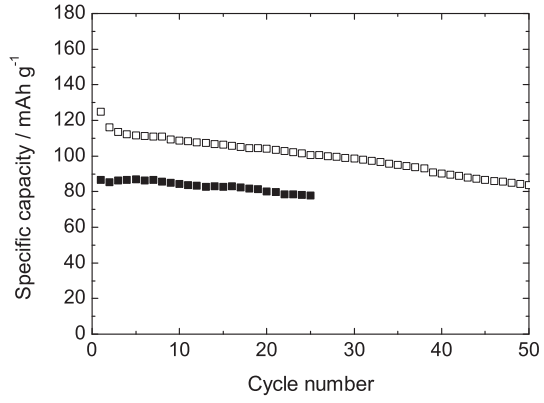

Fig. 9. Specific discharge capacity at 0.1 C *vs.* cycle number at 50 °C (□) and 30 °C (■) of M100(II) electrodes.

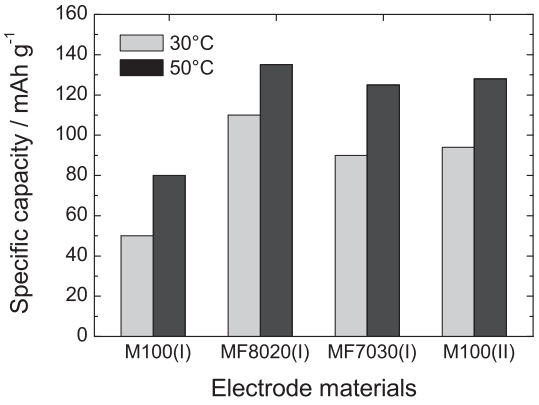

Fig. 10. Comparison of the first discharge capacity of the fully charged electrodes, at 30° and 50 °C.

provides the highest amount of carbon-coating. A summary of the first discharge capacity at 30° and 50 °C for the various electrodes is reported in Fig. 10; the highest operating temperature of 50 °C improves the Li^+ intercalation/deintercalation kinetics with a beneficial impact on the delivered capacity by all the electrodes.

4. Conclusions

Carbon-coated $LiMnPO_4$ and $LiMn_{1-x}Fe_xPO_4$ ($x = 0.2, 0.3$) were prepared from partially water soluble precursors and the former even from totally soluble precursors. Synthesis of $LiMnPO_4$ from totally soluble precursors in stoichiometric ratio, with exclusion of citric acid (2:1), provided an attractive carbon-coated material with the following performance at 0.1 C: 125 mAh g^{-1} at 50 °C and 95 mAh g^{-1} at 30 °C, and a capacity fade per cycle of 0.5% at 50 °C and 0.4% at 30 °C. These results are very promising, particularly in consideration of the inexpensive synthesis procedure, and evidence that a well performing Mn-based olivine is viable, even without the coexistence of iron, and this is an advantage for battery energy because the most charge is delivered at a voltage higher than 3.5 V.

Acknowledgements

The authors wish to thank ENEA and Italy's Ministero dello Sviluppo Economico for financial support under the program "Ricerca di sistema elettrico".

References

[1] A.K. Padhi, K.S. Nanjundaswamy, J.B. Goodenough, Journal of the Electrochemical Society 144 (1997) 1188–1194.
[2] C. Delacourt, et al., Journal of the Electrochemical Society 152 (2005) A913–A921.
[3] M. Yonemura, et al., Journal of the Electrochemical Society 151 (2004) A1352–A1356.
[4] Z. Bakenov, I. Taniguchi, Electrochemistry Communications 12 (2010) 75–78.
[5] J. Xiao, et al., Journal of the Electrochemical Society 157 (2010) A142–A147.
[6] D. Wang, et al., Journal of Power Sources 189 (2009) 624–628.
[7] D. Choi, et al., Nano Letters 10 (2010) 2799–2805.
[8] J. Xiao, et al., Physical Chemistry Chemical Physics 13 (2011) 18099–18106.
[9] H. Ji, et al., Electrochimica Acta 56 (2011) 3093–3100.
[10] K.T. Lee, J. Cho, Nano Today 6 (2011) 28–41.
[11] Y. Dong, et al., Journal of Power Sources 215 (2012) 116–121.
[12] Z. Bakenov, I. Taniguchi, Journal of Power Sources 195 (2010) 7445–7451.
[13] S.-M. Oh, et al., Journal of Alloys and Compounds 506 (2010) 372–376.
[14] T. Shiratsuchi, et al., Electrochimica Acta 54 (2009) 3145–3151.
[15] G. Yang, et al., Journal of Power Sources 196 (2011) 4747–4755.
[16] A. Yamada, Y. Kudo, K.-Y. Liu, Journal of the Electrochemical Society 148 (2001) A747–A754.
[17] H. Wang, et al., Angewandte Chemie International Edition 50 (2011) 7364–7368.